Novel exosome biomarker candidates for Alzheimer´s disease unraveled through Mass Spectrometry analysis

Tânia Soares Martins
IBIMED: Universidade de Aveiro Instituto de Biomedicina
Rui Marçalo
IBIMED: Universidade de Aveiro Instituto de Biomedicina
Cristóvão B. da Cruz e Silva
LIP: Laboratorio de Instrumentacao e Fisica Experimental de Particulas
Dário Trindade
IBIMED: Universidade de Aveiro Instituto de Biomedicina
José Catita
Universidade Fernando Pessoa Faculdade de Ciencias da Saude
Francisco Amado
Universidade de Aveiro Departamento de Quimica
Tânia Melo
Universidade de Aveiro Departamento de Quimica
Ilka Martins Rosa
IBIMED: Universidade de Aveiro Instituto de Biomedicina
Jonathan Vogelgsang
Universitatsmedizin Gottingen
Jens Wiltfang
Universitatsmedizin Gottingen
Odete A. B. da Cruz e Silva
IBIMED: Universidade de Aveiro Instituto de Biomedicina
Ana Gabriela Henriques (aghenriques@ua.pt)
iBiMED - University of Aveiro https://orcid.org/0000-0003-0851-6979

Research

Keywords: Alzheimer’s disease, biomarkers, blood, diagnosis, exosomes, extracellular vesicles

Posted Date: August 18th, 2021

DOI: https://doi.org/10.21203/rs.3.rs-787466/v1

Abstract

Background

Exosomes are small extracellular vesicles (EVs) present in human biofluids that can carry disease-specific molecules. Blood-derived exosomes emerged as interesting peripheral sources of biomarkers for a wide range of diseases, and their potential is also being addressed in Alzheimer's disease (AD) context. There is no effective cure or blood-based molecular diagnostic tools for a first clinical AD screening, which motivates research in this area to identify putative valuable blood-derived disease biomarkers. The ultimate goal is to produce a cost-effective and widely available alternative to the current molecular AD diagnosis that monitors a biomarker triplet in the CSF.

Methods

In the study here presented, EVs with exosome-like characteristics were isolated from the serum of Controls and AD cases through two distinct methods, precipitation- and column-based methods, followed by mass spectrometry analysis. The resulting proteomes from Controls and AD cases were characterized by Gene Ontology (GO) functional enrichment and multivariate analysis. Putative candidate targets identified were validated in distinct cohorts using antibody-based approaches.

Results

Both methodologies isolated particles with the expected morphology and size range. Although GO terms were similar for Controls and AD cases exosomes in both methodologies, the multivariate analysis revealed a clear segregation between Controls and AD cases obtained by the precipitation method. Nine significantly different abundant proteins were identified between Controls and AD cases and exosome levels of AACT and C4BPα, two Aβ-binding proteins, were validated in individuals from independent cohorts.

Conclusions

Serum-derived exosome proteomes were unraveled for the first time in the context of AD through two distinct isolation methodologies, holding disease discriminatory potential. The work carried out gives an important contribution to the identification of novel exosomal biomarker candidates potentially useful as blood-based tools for AD diagnosis.

Background

Alzheimer's disease (AD) is the most common form of dementia worldwide, and the number of individuals affected by this condition is expected to increase exponentially in the next decades. Despite the huge research efforts in the field, no effective treatment or cure is available thus far.

At the histopathological level, AD is characterized by the aggregation and accumulation of the amyloid-beta (Aβ) peptide into senile plaques and of the microtubule-associated protein Tau into neurofibrillary tangles [1], as a

consequence of abnormal phosphorylation events [2, 3]. The accumulation of these disease-associated deposits leads to neuronal death and synaptic dysfunction, as well as glial activation and neuroinflammation, among other neurodegenerative events [4]. Currently, AD diagnosis is supported by clinical symptoms evaluation, brain imaging approaches and, in some cases, by the molecular diagnostic tools available, namely the monitoring of the gold standard biomarker triplet (Aβ, total-Tau and P-Tau 181) in the cerebrospinal fluid (CSF) [5, 6]. This methodology has undeniable value in assisting AD differential diagnosis, nonetheless, it requires a lumbar puncture which is an invasive procedure, thus limiting its wide routine use and its selection as a first screening tool. Hence extensive research has focused on the identification of biomarkers from more easily accessible peripheral biofluids, like blood. Different molecular contents have been tested in this peripheral biofluid, from protein levels to the presence of specific microRNAs [7–9] and even metabolic [10] or lipid profiles [11]. Currently, there are no reliable blood-based biomarkers for AD, but these would be extremely valuable in clinical practice.

Recently, the focus has centered on blood-derived exosomes, a subclass of extracellular vesicles (EVs) with a multivesicular endosomal origin that range from 30–150 nm in diameter. These nanovesicles are formed by the inward budding of endosomes and further released through the fusion of multivesicular bodies with the plasma membrane [12]. Exosomes are secreted by various cell types and can carry relevant proteins, lipids and nucleic acids which reflect the status of the original cells. These type of EVs, present in various body fluids besides blood (e.g., saliva or urine), would represent easily accessible and cost-effective tools as biomarker sources to monitor disease status, but also as drug delivery vehicles for a set of diseases, including cancer, inflammatory and neurological diseases [13]. The lipid bilayer of exosomes ensures the stability of the cargo, protecting the content from enzyme degradation in the bloodstream. In addition, since exosomes are capable of crossing the blood-brain barrier due to their small size, these nanovesicles can be particularly useful to study brain-related disorders [14].

In an AD context, exosomes carry disease specific-related signatures and contribute to the spreading of the amyloidogenic peptide species [9]. The biomarker value of these blood-derived exosomal vesicles has been tested, focusing in particular on the levels of Aβ and other amyloid precursor protein processing species, Tau and phosphorylated tau forms [15–17]. In addition, synaptic proteins, inflammatory mediators, growth factors and lysosomal proteins also present distinct expression pattern in exosomes from AD cases [18–21].

In this work, mass spectrometry (MS) was used to identify new blood-derived exosomal biomarker candidates associated with AD-exosomal proteomes. MS is highly sensitive and, thus, allows an unbiased biomarker identification in biofluids [22]. Proteome profiles were characterized through Gene Ontology analysis, and putative exosomal biomarker candidates were identified and further validated for two distinct patient cohorts. Biomarker candidates that arise from this analysis can constitute novel tools, potentially useful in AD and/or dementia peripheral biofluids-based diagnostics.

Materials And Methods

Study cohorts

Blood samples were collected from individuals enrolled in a primary care-based cohort (pcb-cohort), which comprises volunteer individuals from the Baixo Vouga region of Aveiro. The inclusion and exclusion criteria were defined, and volunteers were submitted to a battery of cognitive tests as previously described [23,24]. The

cognitive and functional performance of volunteers was categorized based on the score obtained in 2 cognitive tests, the Mini-Mental State Examination (MMSE) and the Clinical Dementia Rating (CDR). MMSE scale cut-offs were set according to Portuguese population: 0–2 years of literacy, cutoff = 22; 3–6 years of literacy, cutoff = 24; and ≥7 years of literacy, cutoff = 27. Scores below cutoff indicate possible cognitive impairment (MMSE+) and scores equal or above were classified as normal (MMSE-). CDR scale applied scores between 0 and 3 where 0 accounts for normal, 1 for mild dementia, 2 for moderate and 3 for severe dementia stages.

The pcb-cohort, herein designated as the UA-Cohort, included a subgroup of 32 individuals that scored CDR≥1 and MMSE+ (mean age 77.38±9.17); and 9 clinically reported AD cases (1 AD scored CDR=1, (mean age 78.67±5.07). Sex- and age-matched Controls (MMSE- and CDR=0) were randomly selected from the same cohort (n=32, mean age 76.69±8.07 and n=9, mean age 77.56±4.83).

Another independent cohort, established at the Department of Psychiatry and Psychotherapy at the University Medical Center Goettingen (UMG-Cohort) was also used for biomarker candidate's validation. The UMG-cohort comprises 12 age-matched Controls (mean age 67.58±7.74) and 12 demented individuals clinically diagnosed as ADs (mean age 73.17±10.66) according to the 2011 McKhann criteria, as previously described [25,26]. The UMG-cohort is characterized by neuropsychological testing (CERAD battery testing), and AD diagnosis of these patients is supported by CSF biomarkers (CSF-NDD) and/or PET analysis (amyloid PET and/or FDG-PET). The CSF molecular biomarkers (Total-Tau, Phospho-Tau 181, Aβ42 and Aβ42/Aβ40 ratio) were monitored and cerebral imaging tests were also carried out.-

EVs isolation and characterization

EVs, with exosome-like characteristics, were isolated from serum samples as previously described [10,27,28]. Two distinct exosomes isolation methods were used: the precipitation-based ExoQuick Serum Exosome Precipitation Solution (System Biosciences) (ExoQ) and the column-based Exo-spin Blood Exosome Purification Kit (Cell guidance systems) (ExoS). In brief, serum samples were centrifuged to remove cell debris and then incubated with the respective isolation reagent, followed by a centrifugation step to pellet the nanovesicles. For ExoQ, two exosome isolations were performed: one where the EVs were eluted in PBS for Transmission Electron Microscopy (TEM) and Nanoparticle Tracking Analysis (NTA) and the other where the EVs were resuspended in RIPA for MS and Western blot (WB) analysis. For ExoS, the pellet was ressuspended in PBS, passed through a purification column and eluted with PBS. Part of the resulting EVs was used to perform TEM and NTA; while the remaining EVs suspension was mixed with RIPA buffer with protease inhibitors to lyse the vesicles, allowing subsequent analysis. All exosome-enriched suspensions were aliquoted and stored at -20 °C prior to analyses. Controls and ADs samples were subjected to the same procedure for each EVs isolation method.

Exosome's concentration and size distribution curves were assessed by NTA, using Nanosight NS300^{TM} instrument and NTA 3.2 software (Malvern Instruments, UK), as previously described [27]. NTA analysis was carried out in duplicate for each sample and the particle concentration was corrected by the dilution factor (1:1000).

Exosome-enriched suspensions from both cohorts were randomly selected for TEM analysis [27]. Paraformaldehyde (2%) was added to the exosome suspensions in PBS and then, exosomes were allowed to adsorb in 75 mesh Formvar/carbon grids. A 3% phosphotungstic acid solution was added to perform the

negative staining. TEM images were obtained using a Hitachi H-9000 transmission electron microscope at 300 kV and images were captured using a slow-scan CCD camera.

The protein concentration of exosomal preparations was determined by BCA protein assay and 50 µg of total protein were loaded from each sample, for sodium dodecyl sulphate polyacrylamide gel electrophoresis (SDS-PAGE). Following gel transfer into a nitrocellulose membrane, immunodetection was carried out for the exosomal markers Hsp70, CD63 and RAB11 and for the negative exosomal marker Calnexin. In brief, membranes were blocked in 5% non-fat dry milk and incubated with the primary antibodies: anti-HSP70 (1:500) (SPA-812), anti-CD63 (1:500) (sc-5275), anti-RAB11 (1:500) (610657; BD transduction laboratories), and anti-Calnexin (1:200) (ADI-SPA-860-J). The secondary antibodies used were the anti-mouse (7076S) or anti-rabbit IgG, HRP-linked antibody (7074S) (Cell Signaling Technology) and protein bands were detected using the chemiluminescence reagent ECL Select (GE Healthcare Life Sciences™). Images were acquired with Chemidoc™ gel imaging system (Bio-Rad).

EVs mass spectrometry analysis

For MS analysis, exosomes-like EVs were isolated using ExoQ and ExoS. For each method, serum-derived exosomes were isolated from 5 sex- and age-matched Controls (mean age 77.4±5.41) and 5 clinically diagnosed AD patients (mean age 77.8±5.59) from the UA-cohort. Subsequent biomarker validation was carried out in a higher number of samples from the UA-cohort and from the UMG-cohort.

For MS analyses, EVs preparations in RIPA buffer (ExoQ) or PBS plus RIPA buffer (ExoS) were sonicated and protein was quantified through BCA assay, using Pierce™ BCA Protein Assay kit. Loading buffer (4x) containing β-mercaptoetanol was added to exosomal samples, normalized for protein content (25 µg per sample), and separated in a 5-20% gradient SDS-PAGE. The resulting gels were stained with Coomassie Blue and each individual gel lane was excised and divided into smaller fragments, to facilitate sample digestion. The fragment corresponding to the albumin molecular weight (around 66 kDa) was excluded and thus not analyzed by mass spectrometry. The purpose was to reduce biological sample complexity, containing high levels of albumin, which may interfere with other proteins detection by MS detection. Gel fragments were washed with ammonium bicarbonate and acetonitrile and the proteins were reduced with 10 mM DTT (45 min at 56 ºC) and alkylated with 55 mM iodo-acetamide (30 min at RT). Then, gel pieces were washed again, allowed to dry and rehydrated in digestion buffer containing 12.5 µg/mL^{-1} of sequencing grade modified trypsin in ammonium bicarbonate. Tryptic digestion was performed as previously described [29], with minor modifications. Trypsin was added at an enzyme-to-substrate ratio of 1:30 (w/w) followed by an overnight incubation with 50 mM ammonium bicarbonate at 37ºC. The peptides were extracted by the addition of 5% formic acid (FA, Fluka), 5% FA/50% ACN (20 min each wash, 2x), lyophilized in SpeedVac (Thermo Savant) and peptides were reconstituted in 40 µL 1% FA solution.

Samples were analyzed with a QExactive Orbitrap Mass Spectrometer (Thermo Fisher Scientific, Bremen) through the EASY-spray nano ESI source (Thermo Fisher Scientific, Bremen) that was coupled to an Ultimate 3000 (Dionex, Sunnyvale, CA) HPLC (high-pressure liquid chromatography) system. The trap (5 mm × 300 µm I.d.) and the EASY-spray analytical (150 mm × 75 µm) columns used were C18 Pepmap100 (Dionex, LC Packings) having a particle size of 3 µm. Peptides were trapped at 30 µl/min in 96% solvent A (0.1 % FA). Elution was achieved with the solvent B (0.1 % formic acid/80% acetonitrile v/v) at 300 nl/min. The 92 min gradient

used was as follows: 0–3 min, 96% solvent A; 3–70 min, 4–25% solvent B; 70–90 min, 25–40% solvent B; 90–92 min, 90% solvent B; 90–100 min, 90% solvent B; 101-120 min, 96% solvent A. The mass spectrometer was operated at 1.8 kV in the data dependent acquisition mode. A MS2 method was used with a FT survey scan from 400 to 1600 m/z (resolution 70,000; AGC target 1E6). The 10 most intense peaks were subjected to HCD fragmentation (resolution 17,500; AGC target 5E4, NCE 28%, max. injection time 100 ms, dynamic exclusion 35 s).

MS data analyses

Spectra were processed and analyzed using Proteome Discoverer (version 2.2, Thermo), with the MS Amanda (version 2.0, University of Applied Sciences Upper Austria, Research Institute of Molecular Pathology) and Sequest HT search engines. Uniprot (TrEMBL and Swiss-Prot) protein sequence database (version of October 2017) was used for all searches under *Homo sapiens*. Database search parameters were as follows: carbamidomethylation of cysteine, oxidation of methionine, and the allowance for up to two missed tryptic cleavages. The peptide mass tolerance was 10 ppm and fragment ion mass tolerance was 0.02 Da. To achieve a 1% false discovery rate, the Percolator (version 2.0, Thermo) node was implemented for a decoy database search strategy and peptides were filtered for high confidence and a minimum length of 6 amino acids, and proteins were filtered for a minimum number of peptide sequences of 1. The obtained results were further filtered, applying a cut-off at 1.5-fold increase and another at 0.5-fold decrease. Also, abundances found in less than 2 out of 5 samples were not regarded as being present in the respective condition (AD or Control) and, when no abundance was measured for one of the groups of samples, a 100-fold increase/0.01-fold decrease was considered for the ratio.

Bioinformatic analysis of EVs

Proteomes obtained by MS (gene names from the proteins identified) were initially overlapped through Venn diagrams with a serum exosomal list (Exo Serum list), obtained from databases and from literature search as described in [28], using the Bioinformatics and Evolutionary Genomics website (http://bioinformatics.psb.ugent.be/webtools/Venn/; accessed on 3rd February 2020) to determine the percentage of exosomal proteins present in EVs samples analysed. Only MS proteins for which gene name was available were included in the overlap. From the exosomal proteomes obtained by MS, seven immunoglobulin chains were not included in this analysis since no gene name was available. Additionally, the set of proteins identified for Controls and ADs for each kit by MS (ExoQ and ExoS) was categorized according to their Gene Ontology (GO) annotation, obtained from the UniProt-SwissProt database. The GO terms were filtered according to the Generic GO Slim and categorization was carried out for “Molecular Function” and “Biological Process”.

The protein lists identified by MS were then analyzed through the use of a dedicated software framework (SysBioTK) as previously reported [2], with the exception of the Partial Least Square (PLS) Analysis.

Data was prepared independently for each analysis (AD vs Control for ExoQ; AD vs Control for ExoS). In a first step, the protein abundances obtained from MS were normalized by the median of the protein abundances of the sample. The abundances were then independently transformed for each protein in each sample through the use of the binary logarithm. For some proteins, in some samples, there was no abundance data from MS, regardless that these proteins were not removed. The prepared data was then converted into tabular format and

exported into a text file for later use with Metaboanalyst 4.0 [30] for the Partial Least Square Analysis (PLS) analysis (performed at 11th February 2020), in order to maintain a consistent data set. PLS analysis was performed to evaluate which kit had the highest discriminatory capacity between Controls and AD cases.

To identify proteins with statistically significant differences in abundance, a Welch's t-test with a significance level of 5% (α=0.05) was applied to the mean "normalized and transformed abundance" of the protein in each condition (i.e. the mean across samples for each condition). Volcano plots were created by plotting, for each protein, the p-Value of the Welch's t-test against the fold increase of the mean "normalized and transformed abundance" of the protein. The fold change threshold was set to 2 and a line representing the 5% significance level was drawn.

Heatmaps were created by taking the "normalized abundance" for each protein in each sample. The dendrograms were calculated using the Ward method to cluster similar samples and proteins together. A Euclidian distance metric was used to calculate the distances for the Ward method. The color scale represents the "normalized abundance".

EVs biomarker candidate analyses

Following MS and bioinformatic analysis, biomarker validation was then carried out in a higher number of samples from the UA-cohort and from the UMG-cohort. WB analyses were performed to assess the patterns of two biomarker candidates identified by mass spectrometry: alpha-1-antichymotrypsin (AACT) and C4b-binding protein alpha chain (C4BPα). The protein concentration of exosome samples isolated with ExoQ were determined, and 50 µg of protein were loaded, per sample, in a 5-20% SDS-PAGE followed by proteins transfer to nitrocellulose membranes. Membranes were then blocked with 5% non-fat dry milk and incubated with the primary antibodies anti-AACT (1:500) (sc-59430; Santa Cruz Biotechnology) and anti-C4BPα Antibody (1:500) (sc-398720; Santa Cruz Biotechnology). Subsequently the membranes were incubated with the anti-mouse IgG, HRP-linked antibody (1:2000) (Cell Signaling Technology). Protein bands were detected, as described above, using the chemiluminescence reagent ECL Select (GE Healthcare Life Sciences™) and images were acquired with Chemidoc™ gel imaging system (Bio-Rad). AACT or C4BPα densitometry values for each individual sample were normalized to an exosomal pool loaded in every membrane. Graphs presented express the relative density ratios. Further, AACT and C4BPα levels were also evaluated by enzyme-linked immunosorbent assay (ELISA), in serum-derived exosomes of the same individuals, using the commercial Human AACT ELISA Kit (ab217779; Abcam) or the Human C4 binding protein A ELISA Kit (NBP2-60550; Novus Biologicals), according to manufacturer's instructions. EVs samples were diluted and equal amounts of protein were used for AACT or C4BPα quantification.

Statistical analysis

Statistical analysis were carried out using SPSS version 27 (IBM) or GraphPad Prism 7 (GraphPad Software, La Jolla, California, USA). Data distribution was assessed by Shapiro-Wilk test. Exosomes concentration, mode and the levels of biomarker candidates were compared using unpaired t-tests. Kolmogorov-Smirnov was used to compare the particle size distribution. p-values ≤0.05 were considered significant.

Results

EVs isolation from Controls and AD cases

EVs with exosome-like characteristics were isolated from Control and AD cases using two distinct approaches, precipitation-based (ExoQ) and column-based (ExoS) isolation kits, prior to MS analysis. The exosomes isolated were characterized by Nanoparticle Tracking Analysis (Figure 1A-C). The size distribution curves reveal that both kits isolated vesicles within the expected size range for exosomes. For ExoQ, no differences were found in the particle concentration between Controls ($3.64x10^{11}$±$2.69x10^{11}$ particles/ml) versus AD cases ($3.33x10^{11}$±$2.81x10^{11}$ particles/ml) nor in the mode size between Control and AD group (119.5 ± 17.77 nm and 122.7 ± 18.40 nm, respectively) (Figure 1A-C). In contrast, for ExoS the size distribution of the isolated vesicles and the particle concentration were significantly different ($p \leq 0.05$) between the Control ($6.36x10^{11}$±$2.49x10^{11}$ particles/ml) and AD ($4.41x10^{11}$±$3.15x10^{11}$ particles/ml) groups. No significant differences were found between the mode size of vesicles isolated from Control (112.5±17.32 nm) and AD groups (123.3±28.48 nm). Consistently with NTA, TEM analysis revealed that both methods isolated exosomes with the expected morphology and size (Figure 1D). To confirm the nature of the nanovesicles, western blot analysis was performed. The exosomal markers HSP70, CD63 and RAB11 were detected in the vesicles isolated using ExoQ and ExoS (Figure 1E), while the negative marker Calnexin was not detected, as expected.

GO analyses of EVs from Controls and AD cases

Serum-derived EVs were isolated from Controls and AD cases using both ExoQ and ExoS and then characterized by MS analysis. ExoQ renders in a higher number of proteins identified by MS when compared to ExoS ($p \leq 0.01$). An average number of 127 proteins (mean between data obtained for Controls and ADs) were identified in exosomes-like particles isolated with ExoQ, whereas an average number of 93 proteins were found in exosomes-like particles isolated with ExoS (Table 1 and Supplementary Tables 1 and 2), including protein isoforms. For both kits, AD cases presented a small decrease in the number of proteins identified by MS, although not significantly different. A total of 148 proteins were common to exosomes isolated from both kits, including Controls and ADs proteomes (Supplementary Table 3).

To validate the nature of our samples, exosomal proteomes obtained through MS (gene names of the proteins identified) were overlapped with a serum-derived exosomal gene list. This list was obtained from information recovered from databases, namely Vesiclepedia, EVpedia and Exocarta, to which another 52 proteins (gene names) were also added following a literature review on exosomal AD related proteins [9,28] (Figure 2, Supplementary Table 4 and 5). The majority of the exosomal proteins identified by MS and isolated either with ExoQ and ExoS (66% and 70%, respectively) were also present in the serum-derived exosomal gene list, reinforcing the exosomal nature of the samples. Additionally, novel proteins were found in exosomes isolated from Controls or AD cases, using both kits.

GO functional enrichment analysis was performed to characterize the exosomal-enriched proteome of Controls and AD cases, obtained with ExoQ (Figure 3A-B) or ExoS (Figure 3C-D). The GO terms for molecular function and biological process were similar between Controls and AD cases proteomes obtained from both kits. The top 5 molecular function terms were ion binding, peptidase activity, enzyme regulator activity, structural molecule activity and lipid binding, whereas the top biological process terms in both cases were immune system process, transport, response to stress, vesicle-mediated transport, and signal transduction. In general, ExoQ render in a higher number of proteins isolated and consequently of hits for each category. Interestingly, specific GO terms

could be found, despite the lower number of proteins obtained using the column-based approach. For instance, differences were observed in GO terms for molecular function related to phosphatase and kinase activity, which were found enriched in AD cases compared to Controls for exosomes isolated with ExoQ. For ExoS, an opposite pattern was observed, and Controls were enriched in the GO term for phosphatase activity. These small GO proteomes differences may be interesting if we want to consider addressing a particular process and/or approach during research.

Partial Least Squares analysis of EVs proteomes

PLS analysis was also carried out to assess the performance of the two kits in discriminating Control and AD cases (Figure 4). This analysis revealed that ExoQ presents a higher discriminatory power, as there was no overlap between Controls and AD cases. Taking this evidence into consideration, and the fact that significant differences were obtained in the number of exosome particles isolated from Controls and AD cases, when using ExoS, subsequent analysis were performed highlighting the results obtained with ExoQ in both groups. Nonetheless, data obtained for ExoS was also included as supplementary material.

EVs proteomic signature of Controls and AD cases

Heatmaps were constructed to assess which exosomal proteins could distinguish Controls from AD cases. A total of 279 exosomal proteins were identified with ExoQ among groups. Nonetheless, when using this set of proteins, no clear discrimination between the two groups was achieved with the hierarchical analysis (Supplementary figure 1), since 2 AD cases were classified as Controls. Noticeably, 9 proteins presented significantly different abundance levels between Controls and AD cases. When considering these proteins, the hierarchical analysis correctly discriminated all the individuals (Figure 5).

As depicted in the heatmap (Figure 5) and in the volcano plot (Figure 6), APOC3, APOH, C4BPα, CO3 and KV230 were significantly increased in Control individuals, while AACT Isoform 1, CO9, IGHM Isoform 2 and K2C6A were significantly increased in AD cases. Indeed, 5 of these 9 proteins had already been described as altered in the context of AD (AACT, APOC3, APOH, C4BPα and CO3) (Table 2). Two candidates were selected for subsequent validation: AACT and C4BPα. These were found to be the most interesting candidates since both AACT and C4BPα are detected in senile plaques and both are Aβ-binding proteins [31–34]. AACT can also induce tau phosphorylation [35]. In addition, the patterns of these candidates have been previously addressed in different biofluids, as CSF, plasma and/or serum. Although some inconsistence was observed (Table 2), previous studies also reported similar patterns as those obtained here for serum-derived exosomes through MS. Thus, these candidates with opposite expression patterns in Controls and AD cases, were further validated by WB and ELISA in exosomes.

Heatmaps were also obtained for the exosomal proteome corresponding to the ExoS method and 192 distinct proteins were identified in Control and AD groups, from which 4 proteins showed significant differences for the abundance values among the two groups (HV374, ITIH4 Isoform 1, THRB and HRG) (Supplementary figure 2 and 3, respectively). However, since the disease discriminatory power of this kit was lower than for ExoQ these candidates were not further pursued.

Validation of the putative EVs candidates

To validate the results obtained through MS, the levels of AACT and C4BPα were assessed in exosomal-enriched samples isolated with ExoQ, from both Controls and individuals with dementia from the UA-Cohort but also from Controls and AD cases from the UMG-Cohort. The UA-Cohort study group included samples from sex- and aged-matched Controls (CDR=0 and MMSE-, n=32) and individuals with dementia (CDR≥1 and MMSE+; n=32). This dementia group comprises 10 patients that scored CDR=1 and MMSE+, 22 patients that scored CDR=2&3 and MMSE+ and 9 clinically diagnosed AD cases, of which one scored CDR=1. The UMG-Cohort study group included 12 AD cases and respective aged-matched Controls.

Validation of serum-derived exosomal biomarkers was carried out using WB analysis and ELISA. For AACT, WB analysis showed a tendency for an increase in dementia cases, as observed for the UA-cohort. The mean exosomal levels of AACT were 1.29±0.67 for Controls and 1.65±1.05 for CDR≥1 and MMSE+ (Figure 7A). Regarding AD cases per se, this tendency was also observed, comparatively to the respective sex- and age-matched Controls, although no statistical significance was obtained (1.92±0.81 vs 2.14±1.71, respectively) (Figure 7B). Significant differences were observed however, for the UMG-Cohort, were Controls had lower AACT levels (1.26±0.55) when compared with the AD group (2.12±1.29) ($p \leq 0.05$) (Figure 7C). In accordance, ELISA assays revealed likewise a tendency for increased mean levels of AACT in CDR≥1 and MMSE+ (11336±2532 pg/ml vs 12228±3274 pg/ml) (Figure 7D); and AD groups from both UA-Cohort (12184±3280 pg/ml vs 13948±4728 pg/ml) (Figure 7E) and UMG-Cohort (10703±3114 pg/ml vs 12035±4247 pg/ml) (Figure 7F), comparatively to the Control groups.

As expected, in accordance with the MS analysis results, an opposite pattern was observed for the C4BPα, for both WB and ELISA assays. Comparatively to the Controls, a tendency to lower C4BPα exosomal levels in the CDR≥1 and MMSE+ group (1.01±0.38 vs 0.86±0.24) was obtained by WB analysis (Figure 8A). When considering only the Controls and respective AD cases, C4BPα levels also tend to decrease although with no significant differences (0.94±0.19 and 0.78±0.19) (Figure 8B). Consistently, a tendency for decreased levels of C4BPα in AD group (1.79±0.75) when compared with Controls (1.72±0.64) was likewise observed for the UMG-cohort (Figure 8C). Regarding C4BPα ELISA assays, and comparing against respective Controls, decreased mean levels were obtained for CDR≥1 and MMSE+ (19.62±5.41 ng/ml vs 18.09±5.17 ng/ml) (Figure 8D), and for ADs from UA-Cohort (18.77±4.15 ng/ml vs 17.95±6.15 ng/ml) (Figure 8E). For disease cases from UMG-cohort, this decrease reached statistical significance (20.13±5.24 ng/ml vs 16.51±2.72 ng/ml) ($p \leq 0.05$) (Figure 8F).

Discussion

AD blood-based biomarker candidates will offer less invasive, cheaper and easier alternatives as a first screening to setup in clinical settings or as complementary tools compared to the currently validated biomarker triplet in CSF and imaging approaches. Exosomes have been described as important players in AD pathogenesis, and these EVs can be isolated efficiently from blood, thus constituting important resources in the diagnosis of this pathology. In this work, two distinct methods (precipitation- and column-based methods) were employed to isolate serum-derived EVs, with exosomes like characteristics, from Controls and AD cases, and their proteomes were obtained through MS and characterized. Although, the size and morphology of the EVs obtained were compatible with the expected exosome features, differences in the particle size distribution and in

the number of particles between Controls and AD cases were found for ExoS. Previous studies also reported a tendency for a decreased numbers of particles in AD cases when compared to Control individuals [16]. The distinct particle concentrations did not reflect a significant change in the number of proteins identified through MS, being this very similar between exosomes isolated from Controls and AD cases. Nonetheless, in general, ExoQ rendered in a higher number of proteins when compared with ExoS, which was not surprising since the latter is a column-based approach, and thus more selective. GO analysis reveal that the top 5 biological processes and functions were similar among Controls and disease cases and also between kits. Nonetheless, specific differences in the proteomes and GO analysis were found and should be potentially addressed in the future. Indeed, comparing Controls versus AD cases, the number of hits for phosphatase activity increased in the AD group, for exosomes isolated with ExoQ, whereas the Control group presented more hits for phosphatase activity for exosomes isolated with ExoS. These different patterns may be relevant when choosing exosome isolation approaches, for instance in phosphorylation-related studies, particularly important in the field of AD where abnormal protein phosphorylation is a key event [2, 63, 64].

PLS analysis revealed that ExoQ had a higher disease discriminatory power than ExoS, and for this reason data obtained with this kit were pursued in more detail. A set of 9 proteins presented significantly different abundance levels between Controls and ADs. APOC3, APOH, C4BPα, CO3 and KV230 were significantly decreased in ADs, whereas AACT Isoform 1, CO9, IGHM Isoform 2 and K2C6A, were increased in the exosomes of ADs. Except for IGHM Isoform 2, K2C6A and KV230, all other proteins have already been linked to AD. From those, AACT and C4BPα were considered the most promising candidates to pursue. AACT was an interesting target since it binds Aβ, was found in early stages of senile plaques and promotes its deposition, can induce tau phosphorylation and its levels were correlated with cognitive tests performance [35, 36, 50, 54, 55]. C4BPα was another relevant candidate since it binds the Aβ peptide and can also be found in senile plaques. In addition, it was shown that C4BPα limits the complement activation by Aβ and/or death cells in AD brains, possibly protecting the neuronal environment from immune activation [34]. Moreover, a previous bioinformatic analysis by our group [28] identified both AACT and C4BPα as Aβ-binding proteins in the common exosomal proteome, constructed by the overlap of serum-, plasma- and CSF-exosomal proteomes available in databases such as EXOCARTA, Vesiclepedia or EVpedia. Taken all together, we hypothesized that AACT and C4BPα could represent putative disease exosomal biomarker candidates, and thus both markers were tested in serum-derived exosomes. Western blot and ELISA were employed to validate the exosomal MS results obtained for AACT and C4BPα. The analyses confirmed the candidate biomarkers tendencies in agreement with MS results, although significant differences were only found for AACT and C4BPα when comparing Controls versus AD cases from UMG-Cohort, which was highly characterized by a battery of cognitive and molecular tests. Indeed, some inconsistencies in the levels of these proteins have been reported in AD when using plasma and/or CSF (Table 2), which may relate with the number of individuals enrolled in the study and the distinct techniques used to monitor protein levels. Also, it cannot be excluded that these candidates might also represent early or late-stage biomarkers that alter with disease progression. In support of this, significant correlations were found between AACT exosomal concentrations and MMSE or CDR scores reflecting changes with the cognitive alterations (data not shown). Whether these exosomal biomarkers represent potential candidates for AD diagnosis or general biomarkers for dementia, discriminating the level of cognitive decline, needs to be further validate in a higher number of samples. It would also be interesting to evaluate the levels of these candidates in other neuropathologies, to assess the potential of these two candidates in discriminating AD from other forms of dementia.

Conclusions

Many of the current AD research focus on the finding of novel diagnostic markers in peripheral biofluids like blood. Blood-derived exosomes arise recently as a novel source of disease biomarkers. Data presented identify new exosome putative targets that could distinguish Controls from AD cases. Unravelling the exosome proteome in AD provide a relevant source of blood-based biomarker candidates, easier to implement in the clinical practice, which may represent a wide available tool to assist in AD and/or dementia pre-screening diagnosis.

Abbreviations

AACT: Alpha-1-antichymotrypsin

AD: Alzheimer's disease

Aβ: Amyloid-beta peptide

C4BPα: C4b-binding protein alpha chain

CDR: Clinical Dementia Rating

CSF: Cerebrospinal fluid

ELISA: Enzyme-linked immunosorbent assay

ExoQ: ExoQuick

ExoS: ExoSpin

EVs: Extracellular vesicles

GO: Gene ontology

MMSE: Mini-Mental State Examination

MS: Mass spectrometry

NTA: Nanoparticle tracking analysis

PLS: Partial least square

TEM: Transmission electron microscopy

WB: Western blot

Declarations

Ethics approval and consent to participate: Sample collection as well as their use in research was approved by the ethics committee for health of the Central Regional Administration of Coimbra (CES da ARS Centro, protocol

No. 012804-04.04.2012, Portuguese National Committee for Data Protection (Authorization Nº 369/2012) for the pcb-cohort; and by the ethics committee of the University Goettingen (9/2/16) for the UMG-cohort. All participants provided written informed consent.

Consent for publication: Not applicable.

Availability of data and materials: Data generated or analysed during this study are included in this published article [and its supplementary information files].

Competing interests: The authors declare that they have no competing interests.

Funding: This work was funded by the Alzheimer's Association under Grant 2019-AARG-644347; and also supported by Instituto de Biomedicina (iBiMED) under Grant UIDB/04501/2020; the Fundação para a Ciência e Tecnologia (FCT) of the Ministério da Educação e Ciência, COMPETE program, the QREN and the European Union (Fundo Europeu de Desenvolvimento Regional). JV was funded by the Deutsche Forschungsgemeinschaft (DFG, German Research Foundation) under grant 413501650; TSM is supported by the FCT under the individual PhD grant SFRH/BD/145979/2019. JW is supported by an Ilídio Pinho professorship at University of Aveiro.

Authors' contributions: TSM - conception, design of the work, data acquisition and analysis, interpretation of data, manuscript writing; RM - data acquisition and manuscript revision; CBCS – data analysis, manuscript writing; JC – data acquisition and manuscript revision; FA – data acquisition, analysis, manuscript revision; TM – data acquisition and analysis; IMR – blood samples collection, pcb-cohort characterization; JV – blood samples collection, UMG-Cohort characterization, manuscript revision; JW – blood samples collection, UMG-Cohort characterization, manuscript revision; OABCS – data analysis and manuscript revision; AGH – conception, design of the work, data acquisition and analysis, interpretation of data, manuscript writing. All authors read and approved the final manuscript.

Acknowledgments: We thank the volunteers and their families as well as to all the health professionals involved in this study.

References

1. DeTure MA, Dickson DW. The neuropathological diagnosis of Alzheimer's disease. Mol Neurodegener. 2019;14:32.
2. Henriques AG, Müller T, Oliveira JM, Cova M. da Cruz e Silva CB, da Cruz e Silva OAB. Altered protein phosphorylation as a resource for potential AD biomarkers. Sci Rep. 2016;6:30319.
3. Henriques AG, Vieira SI, da Cruz E. Silva EF, da Cruz e Silva OAB. Aβ promotes Alzheimer's disease-like cytoskeleton abnormalities with consequences to APP processing in neurons. J Neurochem. 2010;113:761–71.
4. Domingues C, da Cruz e Silva OAB, Henriques AG. Impact of Cytokines and Chemokines on Alzheimer's Disease Neuropathological Hallmarks. Curr Alzheimer Res. 2017;14:870–82.
5. Blennow K, Zetterberg H. Cerebrospinal fluid biomarkers for Alzheimer's disease. J Alzheimers Dis. 2009;18:413–7.

6. Welge V, Fiege O, Lewczuk P, Mollenhauer B, Esselmann H, Klafki H-W, et al. Combined CSF tau, p-tau181 and amyloid-β 38/40/42 for diagnosing Alzheimer's disease. J Neural Transm. 2009;116:203–12.
7. Cheng L, Doecke JD, Sharples RA, Villemagne VL, Fowler CJ, Rembach A, et al. Prognostic serum miRNA biomarkers associated with Alzheimer's disease shows concordance with neuropsychological and neuroimaging assessment. Mol Psychiatry. 2015;20:1188–96.
8. Lugli G, Cohen AM, Bennett DA, Shah RC, Fields CJ, Hernandez AG, et al. Plasma Exosomal miRNAs in Persons with and without Alzheimer Disease: Altered Expression and Prospects for Biomarkers. PLoS One. 2015;10:e0139233.
9. Soares Martins T, Trindade D, Vaz M, Campelo I, Almeida M, Trigo G, et al. Diagnostic and therapeutic potential of exosomes in Alzheimer's disease. J Neurochem. 2020;156:162–81.
10. Soares Martins T, Magalhães S, Rosa IM, Vogelgsang J, Wiltfang J, Delgadillo I, et al. Potential of FTIR Spectroscopy Applied to Exosomes for Alzheimer's Disease Discrimination: A Pilot Study. J Alzheimer's Dis. 2020;74:391–405.
11. Su H, Rustam YH, Masters CL, Makalic E, McLean CA, Hill AF, et al. Characterization of brain-derived extracellular vesicle lipids in Alzheimer's disease. J Extracell Vesicles. 2021;10:e12089.
12. Kowal J, Tkach M, Théry C. Biogenesis and secretion of exosomes. Curr Opin Cell Biol. 2014;29:116–25.
13. Armstrong D, Wildman DE. Extracellular Vesicles and the Promise of Continuous Liquid Biopsies. J Pathol Transl Med. 2018;52:1–8.
14. Kanninen KM, Bister N, Koistinaho J, Malm T. Exosomes as new diagnostic tools in CNS diseases. Biochim Biophys Acta. 2016;1862:403–10.
15. Fiandaca MS, Kapogiannis D, Mapstone M, Boxer A, Eitan E, Schwartz JB, et al. Identification of preclinical Alzheimer's disease by a profile of pathogenic proteins in neurally derived blood exosomes: A case-control study. Alzheimers Dement. 2015;11:600-7.e1.
16. Goetzl EJ, Mustapic M, Kapogiannis D, Eitan E, Lobach IV, Goetzl L, et al. Cargo proteins of plasma astrocyte-derived exosomes in Alzheimer's disease. FASEB J. 2016;30:3853–9.
17. Kapogiannis D, Mustapic M, Shardell MD, Berkowitz ST, Diehl TC, Spangler RD, et al. Association of Extracellular Vesicle Biomarkers With Alzheimer Disease in the Baltimore Longitudinal Study of Aging. JAMA Neurol. 2019;76:1340–51.
18. Goetzl EJ, Kapogiannis D, Schwartz JB, Lobach IV, Goetzl L, Abner EL, et al. Decreased synaptic proteins in neuronal exosomes of frontotemporal dementia and Alzheimer's disease. FASEB J. 2016;30:4141–8.
19. Goetzl EJ, Schwartz JB, Abner EL, Jicha GA, Kapogiannis D. High complement levels in astrocyte-derived exosomes of Alzheimer disease. Ann Neurol. 2018;83:544–52.
20. Winston CN, Goetzl EJ, Schwartz JB, Elahi FM, Rissman RA. Complement protein levels in plasma astrocyte-derived exosomes are abnormal in conversion from mild cognitive impairment to Alzheimer's disease dementia. Alzheimers Dement (Amst). 2019;11:61–6.
21. Winston CN, Goetzl EJ, Akers JC, Carter BS, Rockenstein EM, Galasko D, et al. Prediction of conversion from mild cognitive impairment to dementia with neuronally derived blood exosome protein profile. Alzheimers Dement (Amst). 2016;3:63–72.
22. Oeckl P, Otto M. A Review on MS-Based Blood Biomarkers for Alzheimer's Disease. Neurol Ther. 2019;8:113–27.

23. Rosa IM, Henriques AG, Carvalho L, Oliveira J. da Cruz e Silva OAB. Screening Younger Individuals in a Primary Care Setting Flags Putative Dementia Cases and Correlates Gastrointestinal Diseases with Poor Cognitive Performance. Dement Geriatr Cogn Disord. 2017;43:15–28.
24. Rosa IM, Henriques AG, Wiltfang J, da Cruz E, Silva OAB. Putative Dementia Cases Fluctuate as a Function of Mini-Mental State Examination Cut-Off Points. J Alzheimers Dis. 2018;61:157–67.
25. Shahpasand-Kroner H, Klafki H-W, Bauer C, Schuchhardt J, Hüttenrauch M, Stazi M, et al. A two-step immunoassay for the simultaneous assessment of Aβ38, Aβ40 and Aβ42 in human blood plasma supports the Aβ42/Aβ40 ratio as a promising biomarker candidate of Alzheimer's disease. Alzheimers Res Ther. 2018;10:121.
26. Vogelgsang J, Shahpasand-Kroner H, Vogelgsang R, Streit F, Vukovich R, Wiltfang J. Multiplex immunoassay measurement of amyloid-β42 to amyloid-β40 ratio in plasma discriminates between dementia due to Alzheimer's disease and dementia not due to Alzheimer's disease. Exp Brain Res. 2018;236:1241–50.
27. Soares Martins T, Catita J, Martins Rosa I, A. B. da Cruz e Silva O, Henriques AG, da Cruz e Silva OAB, et al. Exosome isolation from distinct biofluids using precipitation and column-based approaches. PLoS One. 2018;13:e0198820.
28. Soares Martins T, Marçalo R, Ferreira M, Vaz M, Silva RM, Rosa IM, et al. Exosomal Aβ-binding proteins identified by "in silico" analysis represent putative blood-derived biomarker candidates for alzheimer´s disease. Int J Mol Sci. 2021;22:3933.
29. Shevchenko A, Tomas H, Havli\[sbreve] J, Olsen JV, Mann M. In-gel digestion for mass spectrometric characterization of proteins and proteomes. Nat Protoc. 2007;1:2856–60.
30. Chong J, Wishart DS, Xia J. Using MetaboAnalyst 4.0 for Comprehensive and Integrative Metabolomics Data Analysis. Curr Protoc Bioinforma. 2019;68:e86.
31. Fraser PE, Nguyen JT, McLachlan DR, Abraham CR, Kirschner DA. Alpha 1-Antichymotrypsin Binding to Alzheimer Aβ Peptides Is Sequence Specific and Induces Fibril Disaggregation In Vitro. J Neurochem. 1993;61:298–305.
32. Gollin PA, Kalaria RN, Eikelenboom P, Rozemuller A, Perry G. α1-Antitrypsin and α1-antichymotrypsin are in the lesions of Alzheimer's disease. Neuroreport. 1992;3:201–3.
33. Sun YX, Wright HT, Janciauskiene S. α1-antichymotrypsin/Alzheimer's peptide Aβ1–42 complex perturbs lipid metabolism and activates transcription factors PPARγ and NFκB in human neuroblastoma (Kelly) cells. J Neurosci Res. 2002;67:511–22.
34. Trouw LA, Nielsen HM, Minthon L, Londos E, Landberg G, Veerhuis R, et al. C4b-binding protein in Alzheimer's disease: binding to Abeta1-42 and to dead cells. Mol Immunol. 2008;45:3649–60.
35. Padmanabhan J, Levy M, Dickson DW, Potter H. Alpha1-antichymotrypsin, an inflammatory protein overexpressed in Alzheimer's disease brain, induces tau phosphorylation in neurons. Brain. 2006;129:3020–34.
36. Vanni S, Moda F, Zattoni M, Bistaffa E, De Cecco E, Rossi M, et al. Differential overexpression of SERPINA3 in human prion diseases. Sci Rep. 2017;7:15637.
37. Abraham CR, Selkoe DJ, Potter H. Immunochemical identification of the serine protease inhibitor α1-antichymotrypsin in the brain amyloid deposits of Alzheimer's disease. Cell. 1988;52:487–501.

38. Licastro F, Mallory M, Hansen LA, Masliah E. Increased levels of α-1-antichymotrypsin in brains of patients with Alzheimer's disease correlate with activated astrocytes and are affected by APOE 4 genotype. J Neuroimmunol. 1998;88:105–10.
39. Licastro F, Parnetti L, Morini M, Davis L, Cucinotta D, Gaiti A, et al. Acute Phase Reactant Alpha 1-antichymotrypsin Is Increased in Cerebrospinal Fluid and Serum of Patients With Probable Alzheimer Disease. Alzheimer Dis Assoc Disord. 1995;9:112–8.
40. Matsubara E, Hirai S, Amari M, Shoji M, Yamaguchi H, Okamoto K, et al. α1-Antichymotrypsin as a possible biochemical marker for Alzheimer-type dementia. Ann Neurol. 1990;28:561–7.
41. Delamarche C, Berger F, Gallard L, Pouplard-Barthelaix A. Aging and Alzheimer's disease: Protease inhibitors in cerebrospinal fluid. Neurobiol Aging Elsevier. 1991;12:71–4.
42. Furby A, Leys D, Delacourte A, Buee L, Soetaert G, Petit H. Are alpha-1-antichymotrypsin and inter-alpha-trypsin inhibitor peripheral markers of Alzheimer's disease? J Neurol Neurosurg Psychiatry. 1991;54:469.
43. Pirttila T, Mehta PD, Frey H, Wisniewski HM. α1-Antichymotrypsin and IL-1β are not increased in CSF or serum in Alzheimer's disease. Neurobiol Aging. 1994;15:313–7.
44. Lanzrein AS, Johnston CM, Perry VH, Jobst KA, King EM, Smith AD. Longitudinal study of inflammatory factors in serum, cerebrospinal fluid, and brain tissue in Alzheimer disease: Interleukin-1β, interleukin-6, interleukin-1 receptor antagonist, tumor necrosis factor-α, the soluble tumor necrosis factor receptors I and I. Alzheimer Dis Assoc Disord. 1998;12:215–27.
45. Lawlor BA, Swanwick GRJ, Feighery C, Walsh JB, Coakley D. Acute phase reactants in Alzheimer's disease. Biol Psychiatry Elsevier USA. 1996;39:1051–2.
46. Matsubara E, Amari M, Shoji M, Harigaya Y, Yamaguchi H, Okamoto K, et al. Serum concentration of alpha 1-antichymotrypsin is elevated in patients with senile dementia of the Alzheimer type. Prog Clin Biol Res. 1989;317:707–14.
47. Brugge K, Katzman R, Hill LR, Hansen LA, Saitoh T. Serological α1-Antichymotrypsin in Down's syndrome and Alzheimer's disease. Ann Neurol. 1992;32:193–7.
48. Altstiel LD, Lawlor B, Mohs R, Schmeidler J, Dalton A, Mehta P, et al. Elevated alpha1-antichymotrypsin serum levels in a subset of nondemented first-degree relatives of Alzheimer's disease patients. Dement Geriatr Cogn Disord. 1995;6:17–20.
49. Lieberman J, Schleissner L, Tachiki KH, Kling AS. Serum α1-antichymotrypsin level as a marker for Alzheimer-type dementia. Neurobiol Aging. 1995;16:747–53.
50. DeKosky ST, Ikonomovic MD, Wang X, Farlow M, Wisniewski S, Lopez OL, et al. Plasma and cerebrospinal fluid α1-antichymotrypsin levels in Alzheimer's disease: Correlation with cognitive impairment. Ann Neurol. 2003;53:81–90.
51. Nielsen HM, Minthon L, Londos E, Blennow K, Miranda E, Perez J, et al. Plasma and CSF serpins in Alzheimer disease and dementia with Lewy bodies. Neurology. 2007;69:1569–79.
52. Porcellini E, Davis E, Chiappelli M, Ianni E, Di Stefano G, Forti P, et al. Elevated Plasma Levels of alpha-1-Anti-Chymotrypsin in Age-Related Cognitive Decline and Alzheimers Disease: A Potential Therapeutic Target. Curr Pharm Des. 2008;14:2659–64.
53. Licastro F, Pedrini S, Caputo L, Annoni G, Davis LJ, Ferri C, et al. Increased plasma levels of interleukin-1, interleukin-6 and α-1-antichymotrypsin in patients with Alzheimer's disease: Peripheral inflammation or

signals from the brain? J Neuroimmunol. 2000;103:97–102.
54. Nilsson LNGG, Bales KR, DiCarlo G, Gordon MN, Morgan D, Paul SM, et al. α-1-Antichymotrypsin Promotes β-Sheet Amyloid Plaque Deposition in a Transgenic Mouse Model of Alzheimer's Disease. J Neurosci. 2001;21:1444–51.
55. Tyagi E, Fiorelli T, Norden M, Padmanabhan J. Alpha 1-Antichymotrypsin, an Inflammatory Protein Overexpressed in the Brains of Patients with Alzheimer's Disease, Induces Tau Hyperphosphorylation through c-Jun N-Terminal Kinase Activation. Int J Alzheimers Dis. 2013;2013:1–11.
56. Shih Y-HH, Tsai K-JJ, Lee C-WW, Shiesh S-CC, Chen W-TT, Pai M-CC, et al. Apolipoprotein C-III is an Amyloid-β-Binding Protein and an Early Marker for Alzheimer's Disease. J Alzheimers Dis. 2014;41:855–65.
57. Öhrfelt A, Andreasson U, Simon A, Zetterberg H, Edman Å, Potter W, et al. Screening for New Biomarkers for Subcortical Vascular Dementia and Alzheimer's Disease. Dement Geriatr Cogn Dis Extra. 2011;1:31–42.
58. Fei S, Anne P, John C, Nicole AK, Wei W, Barbara C, et al. Plasma Apolipoprotein Levels Are Associated With Cognitive Status and Decline in a Community Cohort of Older Individuals. PLoS One. 2012;7:e34078.
59. Song F, Poljak A, Kochan NA, Raftery M, Brodaty H, Smythe GA, et al. Plasma protein profiling of Mild Cognitive Impairment and Alzheimer's disease using iTRAQ quantitative proteomics. Proteome Sci. 2014;12:5.
60. Castora FJ, Conyers BL, Gershon BS, Kerns KA, Campbell R, Simsek-Duran F. The T9861C Mutation in the mtDNA-Encoded Cytochrome C Oxidase Subunit III Gene Occurs in High Frequency but with Unequal Distribution in the Alzheimer's Disease Brain. J Alzheimers Dis. 2019;72:257–69.
61. Loeffler DA, Camp DM, Bennett DA. Plaque complement activation and cognitive loss in Alzheimer's disease. J Neuroinflammation. 2008;5:9.
62. Yasojima K, Schwab C, McGeer EG, McGeer PL. Up-regulated production and activation of the complement system in Alzheimer's disease brain. Am J Pathol. 1999;154:927–36.
63. Oliveira J, Costa M, de Almeida MSC, da Cruz E, Silva OAB, Henriques AG. Protein Phosphorylation is a Key Mechanism in Alzheimer's Disease. J Alzheimers Dis. 2017;58:953–78.
64. Oliveira JM, da Cruz E, Silva CB, Müller T, Martins TS, Cova M, da Cruz E, Silva OAB, et al. Toward Neuroproteomics in Biological Psychiatry: A Systems Approach Unravels Okadaic Acid-Induced Alterations in the Neuronal Phosphoproteome. OMICS. 2017;21:550–63.

Tables

Table 1

	ExoQ		ExoS	
	Controls	AD	Controls	AD
Mean±SD	136.8±7.5	117.8±29.5	100.2±8.0	85.8±16.6

Table 2

	Gene	Protein name	Alteration in AD	Involvement in AD pathogenesis	Biofluid/brain	Publication
ExoQ	AACT	α-1-antichymotrypsin (SERPINA3)	↑	Present at amyloid plaques.	Human brain	[35–38]
			↑		CSF and Serum	[39,40]
			=		CSF and serum	[41–44]
			=		Serum	[45]
			↑		Serum	[46–49]
			↑		CSF and Plasma	[50,51]
			↑		Plasma	[52,53]
				Promotes Aβ plaques deposition.	Transgenic mice brain	[54]
				Induce tau hyperphosphorylation.	Transgenic mice brain	[35,55]
	APOC3	Apolipoprotein C-III	↓		Plasma	[56]
	APOH	Beta-2-glycoprotein 1	↑		CSF	[57]
			↓ in ApoE4 carriers and MCI individuals		Plasma	[58]
	C4BPα	C4b-binding protein alpha chain*		Detected in Abeta plaques and apoptotic cells.	Human brain	[34]
			=		CSF and Plasma	
				Bind to Aβ through α chain; limits the complement activation on Aβ peptide.	in vitro	
			↓		Plasma	[59]
	CO3	Cytochrome c oxidase subunit 3		AD brains can have a mutation point in the CO3 that changes phenylalanine to leucine. In AD brains with this mutation there is a reduction of CO/citrate synthase activity.	Human brain	[60]

CO9	Complement component C9	↑	Increased number of C9-stained difuse plaques in AD vs C or MCI.	Post-mortem human brain specimens	[61]
		↑		Human brain	[62]
		C5b-C9 ↑		Plasma-derived exosomes	[19]
IGHM	Immunoglobulin heavy constant mu	-	-	-	-
K2C6A	Keratin, type II cytoskeletal 6A	-	-	-	-
KV230	Immunoglobulin kappa variable 2-30	-	-	-	-

Figures

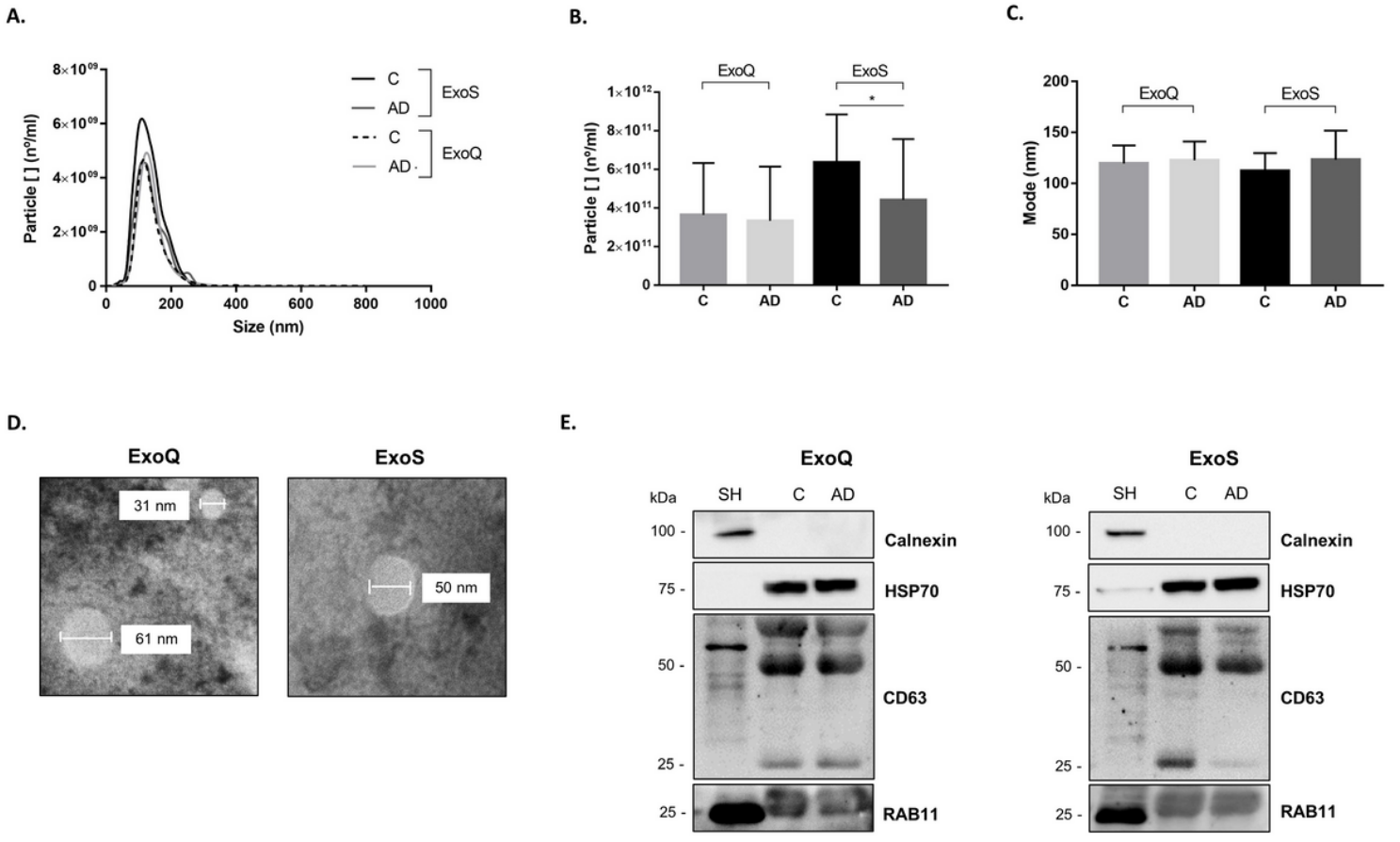

Figure 1

Characterization of blood-derived EVs isolated using ExoQ and ExoS. Exosome-like EVs size distribution (A), particle concentration (B) and mode size (C) determined by Nanoparticle Tracking Analysis. (D) Transmission Electron Microscopy of isolated nanovesicles and (E) Western blot analysis of the exosomal markers HSP70, CD63 and RAB11. Abbreviations: ExoQ, ExoQuick; ExoS, Exo-spin; SH, SH-SY5Y lysates.

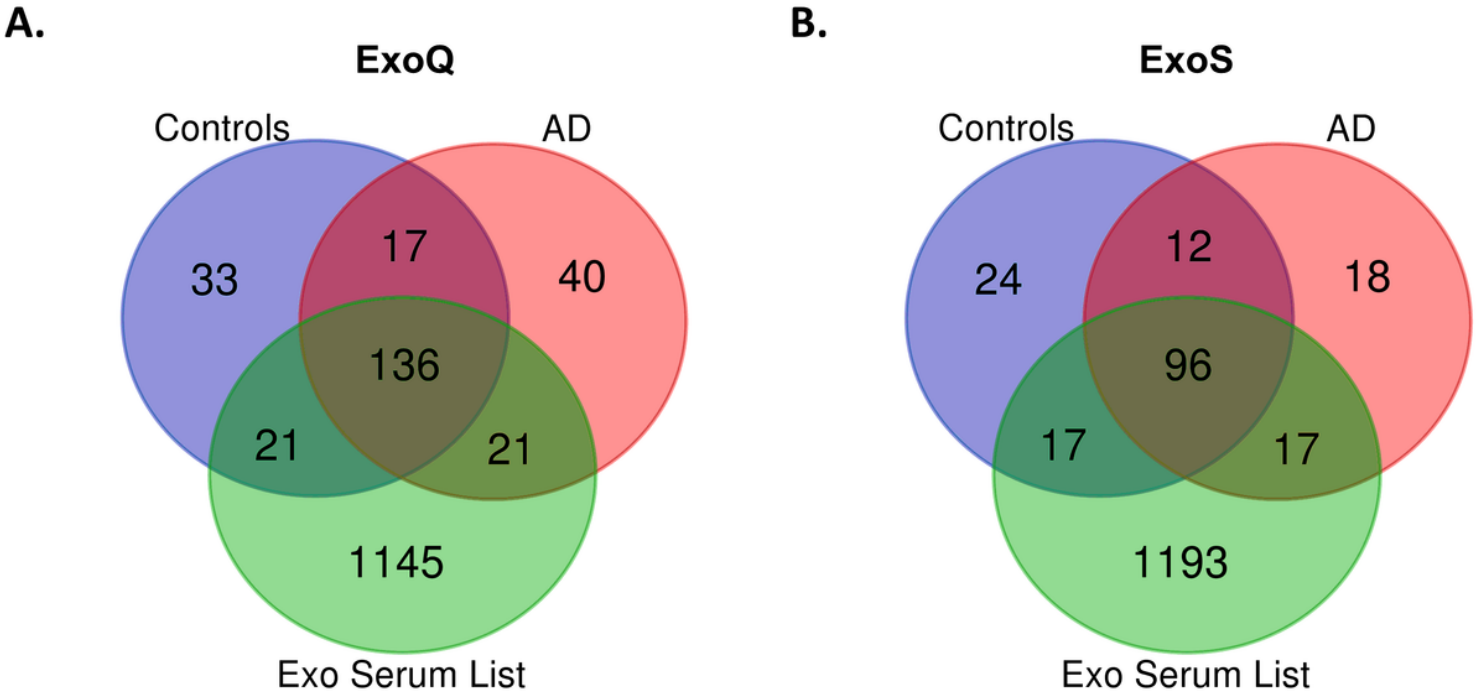

Figure 2

Overlap of exosomal-enriched proteomes obtained by MS with serum-derived exosomal database recovered list. Venn diagrams illustrating the overlap of the exosomal-enriched proteomes obtained by MS (gene names of the proteins identified) after exosome isolation with ExoQ (A) and ExoS (B) with serum exosomal gene names (Exo Serum List) obtained from databases and literature search. Abbreviations: ExoQ, Exoquick; ExoS, Exo-spin.

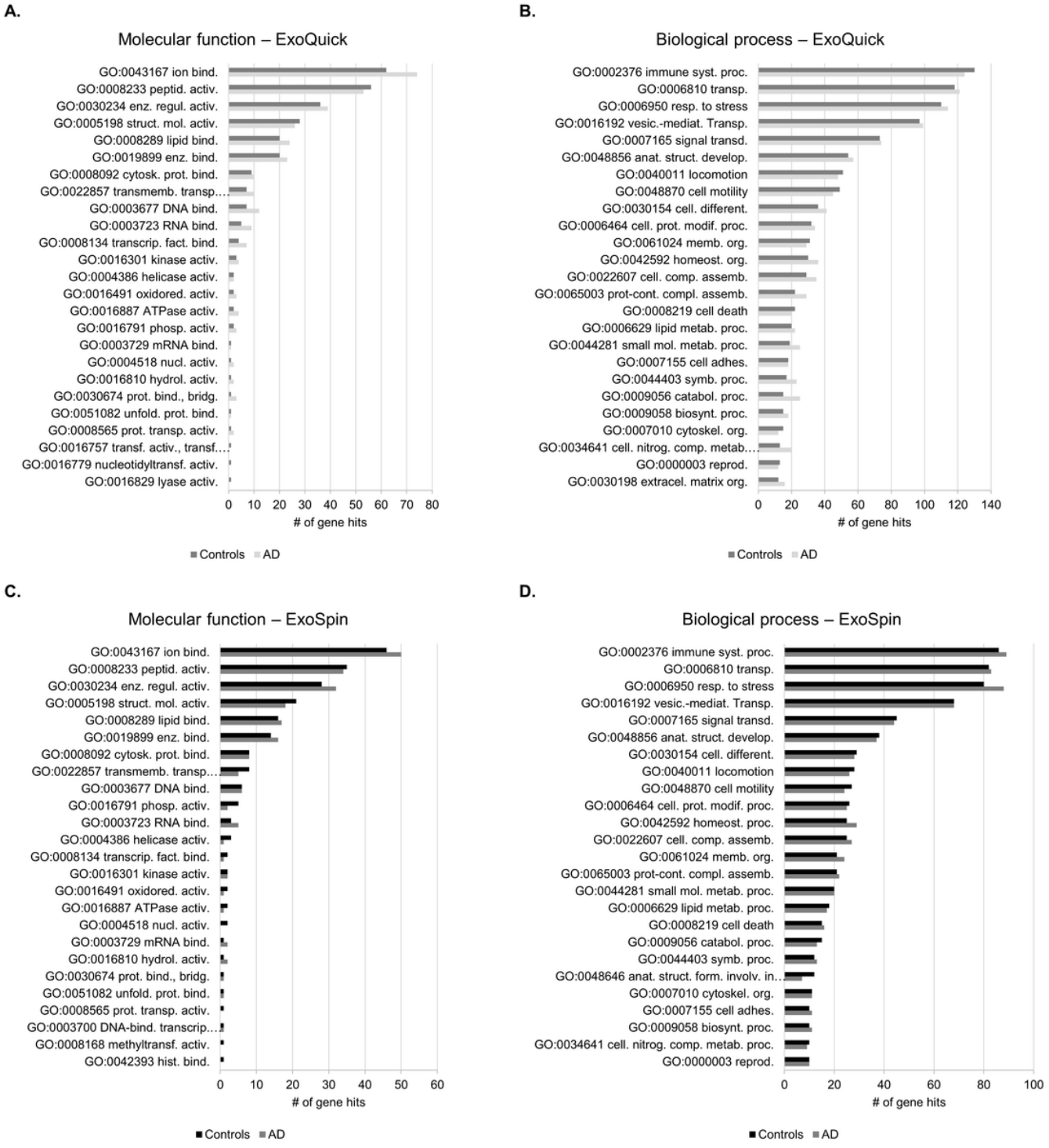

Figure 3

GO analysis of Controls and ADs exosomal-enriched proteomes obtained with ExoQ or ExoSpin. The top 25 molecular function and biological processes terms were annotated for exosomes isolated with ExoQuick (A and B) or ExoSpin (C and D). Dark grey bars represent Controls and light grey represent AD cases. Abbreviations: ExoQ, ExoQuick; ExoS, ExoSpin. Abbreviations of GO molecular function: GO:0043167, ion binding; GO:0008233, peptidase activity; GO:0030234, enzyme regulator activity; GO:0005198, structural molecule activity; GO:0008289, lipid binding; GO:0019899, enzyme binding; GO:0008092, cytoskeletal protein binding; GO:0022857, transmembrane transporter activity; GO:0003677, DNA binding; GO: 0003723, RNA binding;

GO:0008134, transcription factor binding; GO:0016301, kinase activity; GO:0004386, helicase activity; GO:0016491, oxidoreductase activity; GO:0016887, ATPase activity; GO:0016791, phosphatase activity; GO:0003729, mRNA binding; GO:0004518, nuclease activity; GO:0016810, hydrolase activity, acting on carbon-nitrogen (but not peptide) bonds; GO: 0030674, protein binding, bridging; GO:0051082, unfolded protein binding; GO:0008565, protein transporter activity; GO:0016757, transferase activity, transferring glycosyl groups; GO:0016779, nucleotidyltransferase activity; GO:0016829, lyase activity; GO:0003700, DNA-binding transcription factor activity; GO:0008168, methyltransferase activity; GO:0042393, histone binding. Abbreviations of GO biological process: GO:0002376, immune system process; GO:0006810, transport; GO:0006950, response to stress; GO:0016192, vesicle-mediated transport; GO:0007165, signal transduction; GO:0048856, anatomical structure development; GO:0040011, locomotion; GO:0048870, cell motility; GO:0030154, cell differentiation; GO:0006464, cellular protein modification process; GO:0061024, membrane organization; GO:0042592, homeostatic process; GO:0022607, cellular component assembly; GO:0065003, protein-containing complex assembly; GO:0008219, cell death; GO:0006629 lipid metabolic process; GO:0044281, small molecule metabolic process; GO:0007155, cell adhesion; GO:0044403, symbiont process; GO:0009056, catabolic process; GO:0009058, biosynthetic process; GO:0007010, cytoskeleton organization; GO:0034641, cellular nitrogen compound metabolic process; GO:0000003, reproduction; GO:0030198, extracellular matrix organization; GO:0048646, anatomical structure formation involved in morphogenesis.

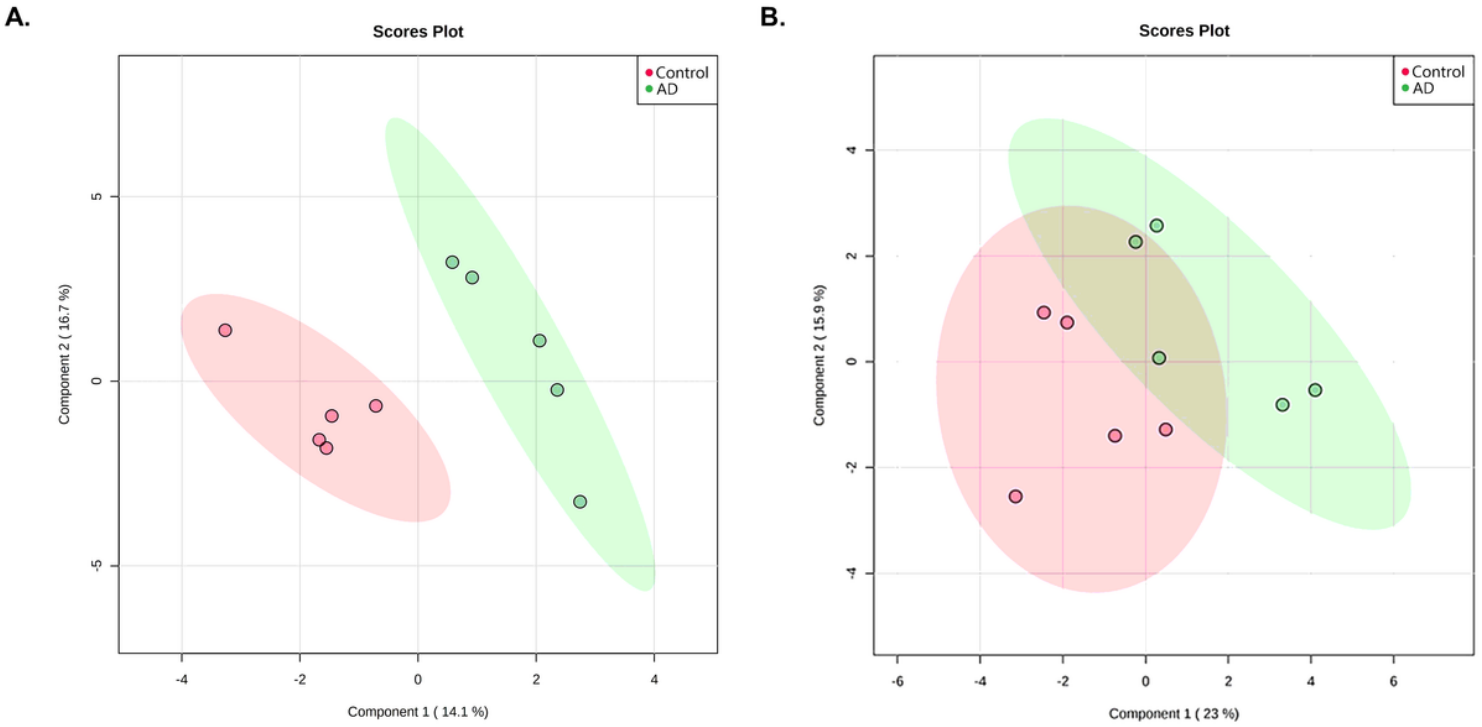

Figure 4

Partial least squares analysis of EVs proteomes of Controls and AD cases. EVs preparations with exosome-like characteristics were isolated with ExoQ (A) or ExoS (B). Green and pink areas represent the 95% confidence region. Abbreviations: ExoQ, ExoQuick; ExoS, Exo-spin.

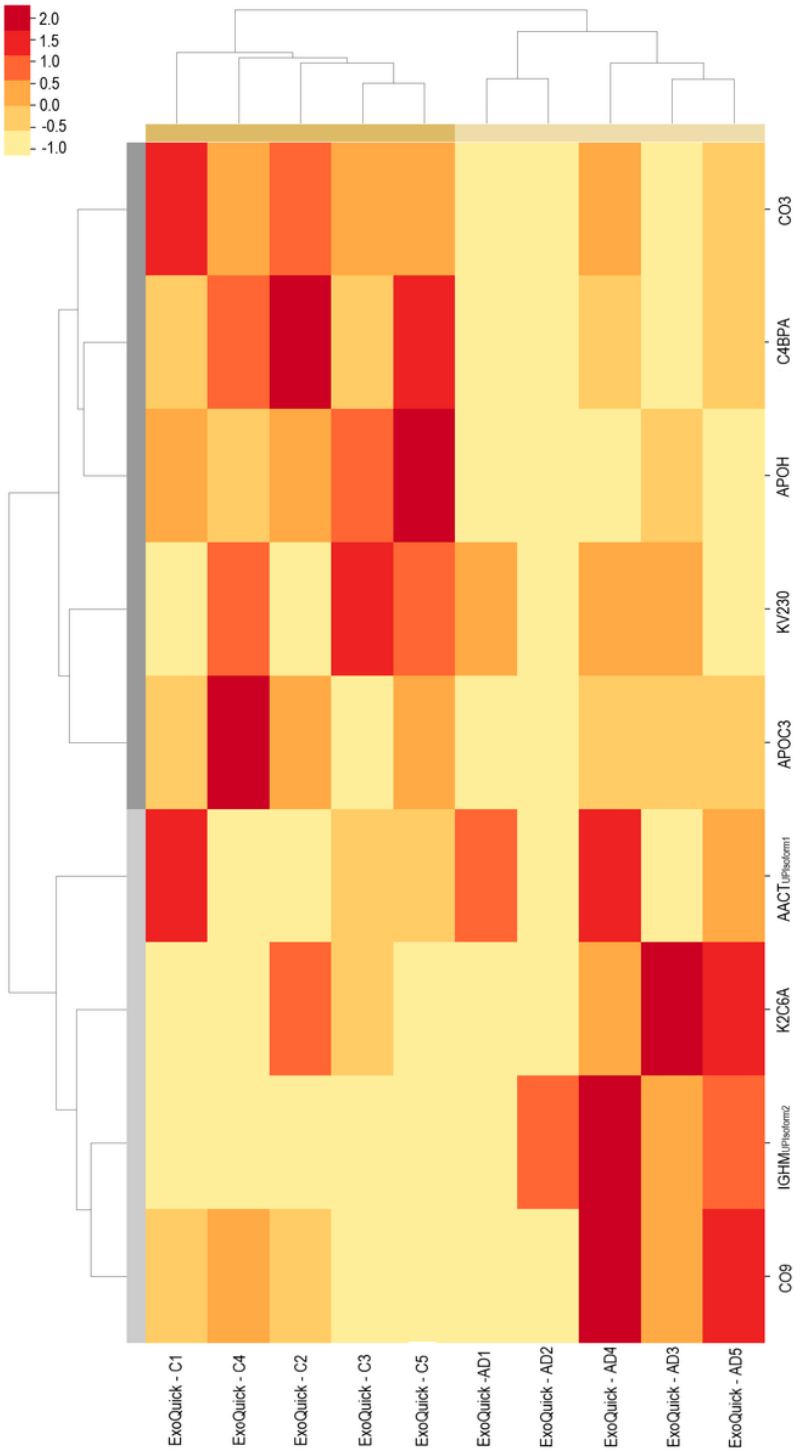

Figure 5

Heatmap of exosomal proteome abundance changes in disease. Heatmaps were constructed for the proteome of significant different proteins in Controls vs AD. Differences were determined using Welch's t-test and a 95% confidence level was considered. The bars on the top of heatmaps show the kits category. Red represents higher abundance and light yellow represents lower abundance levels. UniProt protein names and isoforms are indicated at the right. Abbreviations: C, Controls; AD, Alzheimer's disease; ExoQ, ExoQuick; UP, UniProt.

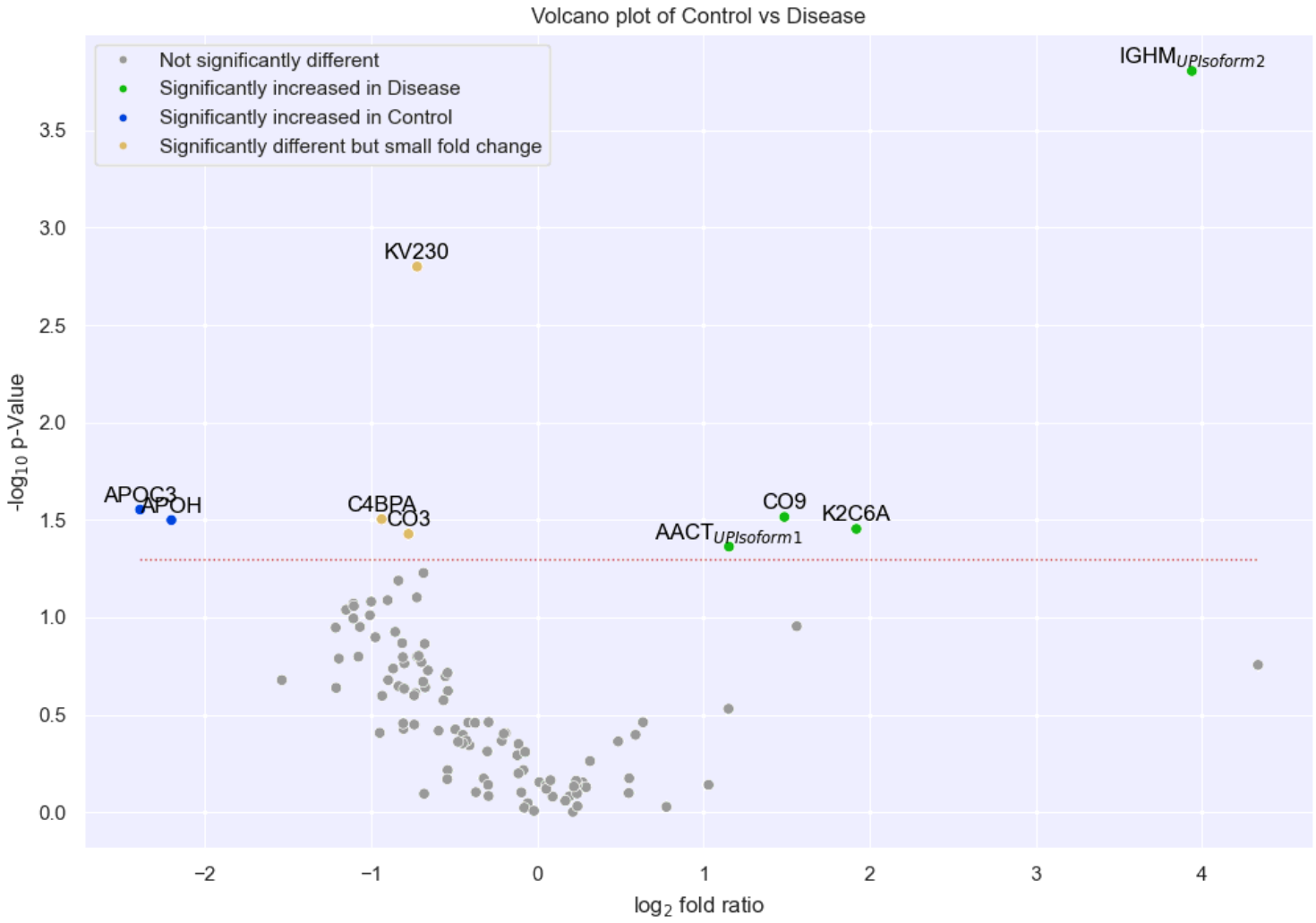

Figure 6

Volcano plot of significant different exosomal proteins in Control and AD cases. Exosomes were isolated using ExoQuick. The dashed red line indicates the p-value threshold of 0.05.

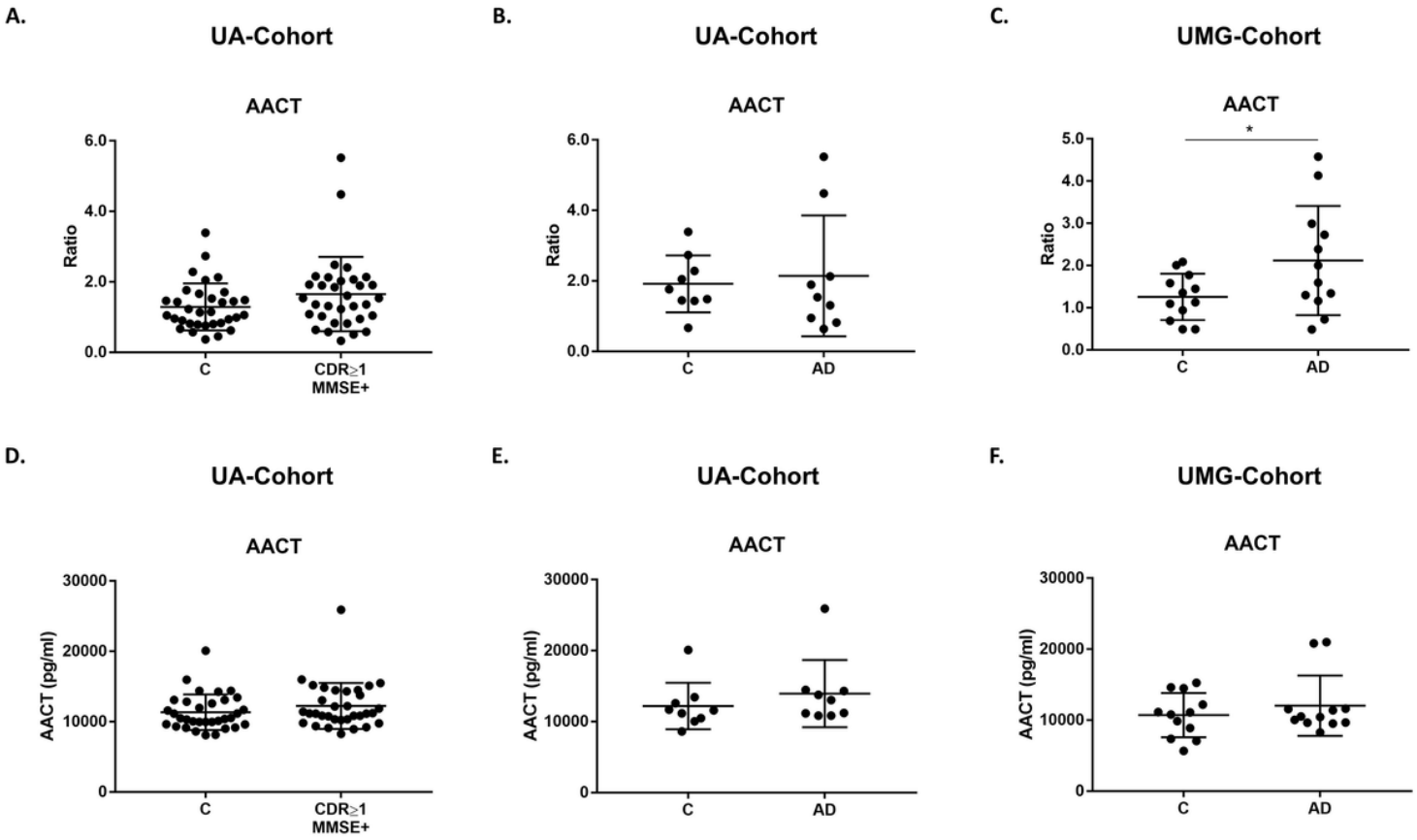

Figure 7

AACT exosomal levels in dementia and AD cases monitored by distinct antibody-based approaches. AACT levels were assessed through immunoblot analysis or commercial ELISA assays in serum-derived exosomes from Controls (CDR=0 and MMSE-) and individuals with dementia (CDR≥1 and MMSE+) from UA-Cohort (A, D), and AD clinically diagnosed cases from UA-Cohort (B, E) or UMG-Cohort (C, F). For WB, each point represents the relative densitometry ratio. For ELISA, each point represents the mean concentration value obtained for each individual. The solid horizontal line shows mean, and error bars indicates standard deviations. Abbreviations: AD, Alzheimer's disease; C, Controls; CDR, Clinical Dementia Rate; MMSE, Mini-Mental State Examination. *p≤0.05

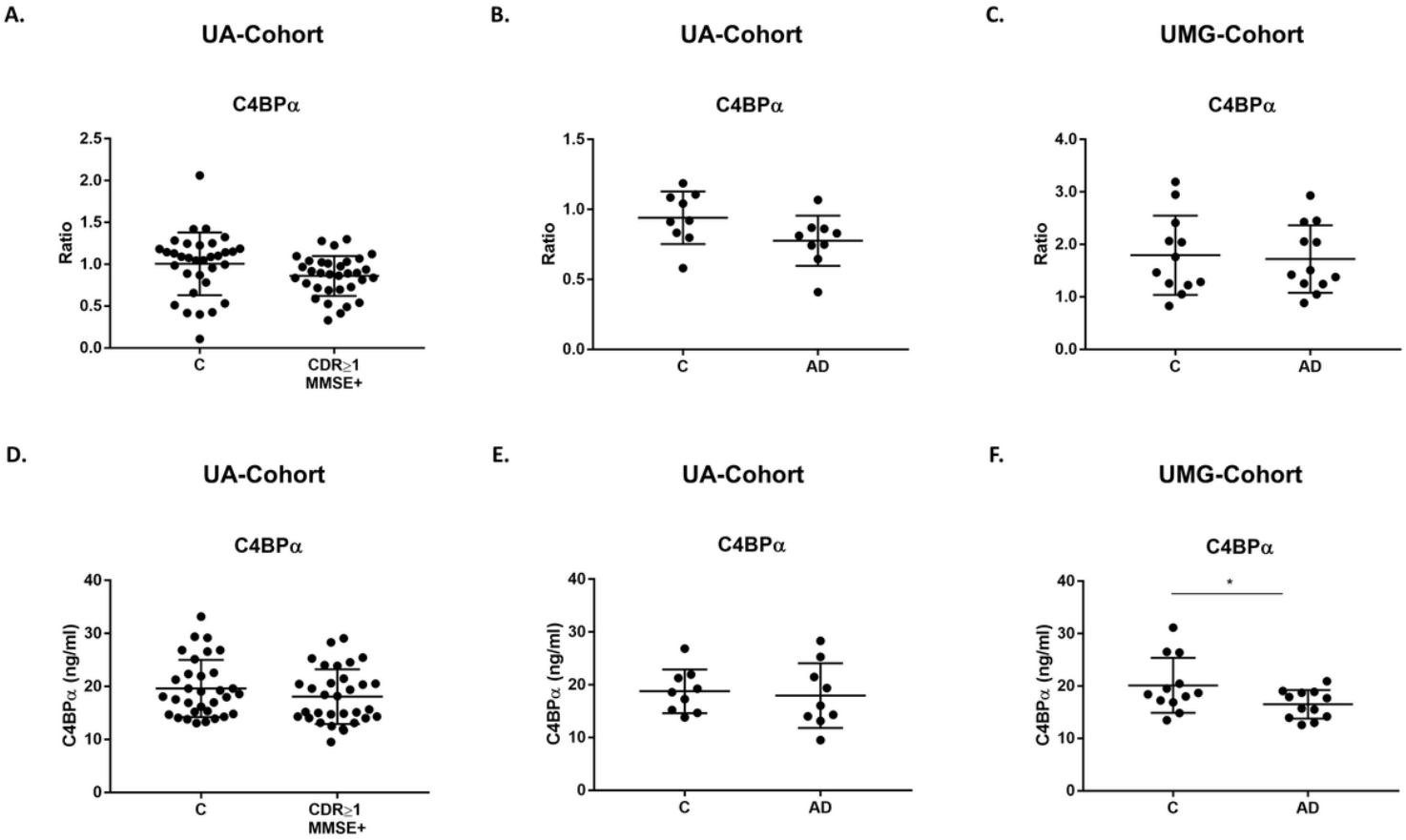

Figure 8

C4BPα exosomal levels in dementia and AD cases monitored by distinct antibody-based approaches. C4BPα levels were assessed through immunoblot analysis or commercial ELISA assays in serum-derived exosomes from Controls (CDR=0 and MMSE-) and individuals with dementia (CDR≥1 and MMSE+) from UA-Cohort (A, D), and AD clinically diagnosed cases from UA-Cohort (B, E) or UMG-Cohort (C, F). For WB, each point represents the relative densitometry ratio, and, for ELISA, it represents the mean concentration value obtained for each individual. The solid horizontal line shows mean, and error bars indicates standard deviations. Abbreviations: AD, Alzheimer's disease; C, Controls; CDR, Clinical Dementia Rate; MMSE, Mini-Mental State Examination. *p≤0.05

Supplementary Files

This is a list of supplementary files associated with this preprint. Click to download.

- Supplementaryfiguresandtablesvf.docx